

Electric Stimulation Parameters for an Epi-Retinal Prosthesis

by

Andrew Eli Grumet

Submitted to the Department of Electrical Engineering and Computer Science

in partial fulfillment of the requirements for the degree of

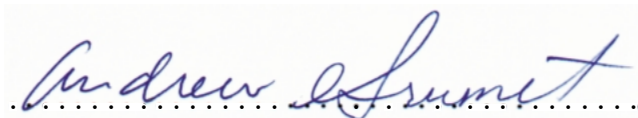
Doctor of Philosophy

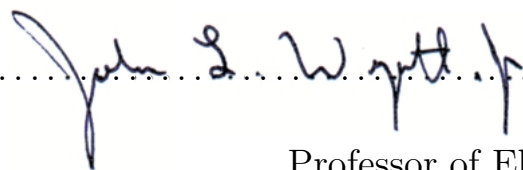
at the

MASSACHUSETTS INSTITUTE OF TECHNOLOGY

September 1999

© Massachusetts Institute of Technology 1999. All rights reserved.

Author 
Department of Electrical Engineering and Computer Science
August 26, 1999

Certified by  8/26/99
John L. Wyatt, Jr.
Professor of Electrical Engineering
Thesis Supervisor

Accepted by 
Arthur C. Smith
Chairman, Department Committee on Graduate Students

Electric Stimulation Parameters for an Epi-Retinal Prosthesis

by
Andrew Eli Grumet

Submitted to the Department of Electrical Engineering and Computer Science
on August 26, 1999, in partial fulfillment of the
requirements for the degree of
Doctor of Philosophy

Abstract

This work was undertaken to contribute to the development of an epi-retinal prosthesis which may someday restore vision to patients blinded by outer retinal degenerations like retinitis pigmentosa. By stimulating surviving cells in tens or hundreds of distinct regions across the retinal surface, the prosthesis might convey the visual scene in the same way that images are represented on a computer screen. The anatomical and functional arrangement of retinal neurons, however, poses a potential obstacle to the success of this approach. Stimulation of ganglion cell axons—which lie in the optic nerve fiber layer between stimulating electrodes and their intended targets, and which originate from a relatively diffuse peripheral region—would probably convey the perception of a peripheral blur, detracting from the usefulness of the imagery.

Inspired by related findings in brain and peripheral nerve stimulation, experiments were performed in the isolated rabbit retina to determine if excitation thresholds for ganglion cell axons could be raised by orienting the stimulating electric field perpendicularly to the axons' path. Using a custom-designed apparatus, axon (and possibly dendrite) thresholds were measured for stimulation through a micro-fabricated array of disk electrodes each having a diameter of ten microns. The electrodes were driven singly versus a distant return (monopolar stimulation) and in pairs (bipolar stimulation) oriented along fibers (longitudinal orientation) or across fibers (transverse orientation). Transverse thresholds were measured for a range of fiber displacements between the two poles of the bipolar electrode pair, and compared in each case with the monopolar threshold for the closer pole. Transverse/monopolar threshold ratios were near unity when one of the poles was directly over the fiber, but rose rapidly with improved centering of the bipolar pair. Longitudinal/monopolar threshold ratios were near unity over the same range of displacements.

As in previous work by others, thresholds were highest for perpendicular stimulating fields. Practical application of this result will require electrode designs which minimize longitudinal fringing fields.

Thesis Supervisor: John L. Wyatt, Jr.
Title: Professor of Electrical Engineering

Acknowledgments

I arrived at MIT in the summer of 1992 with decided interests in analog circuit design and neuroscience, but no funding. To get the ball rolling, I showed up early, sublet an apartment in Inman Square and started making phone calls. It wasn't long after my arrival that I walked into John Wyatt's office. He was easily the friendliest person I had met at MIT up to that point, and his retinal implant research sounded interesting. Within forty-eight hours of our first meeting, I had an office, a desk, a computer account, and a summer research project with no strings attached. What a welcome!

Ultimately the summer job evolved into a doctoral dissertation. Along the way John has been an advisor, a teacher, a colleague, and a friend. His thoughtfulness and optimism have been a continual inspiration, often keeping me going when progress was slow. Of course, it's hard to work closely with someone for seven years and agree on *everything*. But we've always managed to find a mutually acceptable way out when disagreements arose. I truly could not have hoped for a better graduate school experience. First off, then, I want to thank John for giving me absolutely nothing to complain about.

Dr. Joe Rizzo, a co-director with John of the larger project encompassing my work, has been a valued mentor and friend, and read an early version of this document.

Tom Weiss advised me against doing an experimental thesis from scratch, but—to my great benefit—still participated on my thesis committee even when I didn't take his advice. In addition, his clear and incisive presentations of technical material have served as a model which I have endeavored for many years to emulate in my own work.

Don Eddington, in addition to participating on my thesis committee, provided support and guidance at pivotal points along the way.

Dennis Freeman supported my work in many ways, most notably by letting me use all of the neat equipment in “the chemistry room”.

Without the help of Markus Meister and Richard Masland, I would never have gotten the experimental setup working as quickly as I did. David Warland and Iman Brivanlou at the Meister lab were especially helpful.

Malini Narayanan, Sumiko Miller Goldbaum, Alan Gale, Tim Denison, Shawn Kelly, Brad Lichtenstein, and Erich Caulfield all worked in the same lab with me at various times, and as a result shared (whether they were in a loquacious mood or not) in many a good laugh and deep discussion.

Mohamed Shahin provided invaluable assistance with the experiments.

The Whitaker Foundation generously picked up the tab for roughly half of my tuition and stipend, and also provided some greatly appreciated discretionary funds for textbooks and travel.

Finally, I'd like to acknowledge my family and my wonderful wife, Lara Asmundson, for their moral support through high and low.

Contents

1	Introduction	11
1.1	Background and motivation	11
1.1.1	Neural and retinal prostheses	11
1.1.2	Electric stimulation parameters	12
1.1.3	Objective	13
1.2	Related work	13
1.2.1	Direct threshold comparisons	15
1.2.2	Indirect threshold comparisons	15
1.2.3	The pulse duration hypothesis	17
1.2.4	Other studies	19
1.2.5	Discussion	19
1.3	What's In This Thesis	20
2	Multi-Electrode Stimulation and Recording In the Isolated Retina	21
2.1	Introduction	21
2.2	<i>In vitro</i> preparation	22
2.3	Electrode array design	23
2.3.1	Cross-section	26
2.3.2	Electrode layout	26
2.3.3	Electrical connections to instruments	27
2.4	Data acquisition	27
2.4.1	Multi-channel nerve response amplifier	27
2.4.2	Stimulator	28
2.4.3	Computer interface	28
2.4.4	Oscilloscope and speakers	29
2.4.5	Reducing stimulus artifacts	29
2.5	Physiologic recordings	30
2.5.1	Spontaneous and light-evoked activity	30
2.5.2	Electrically evoked activity	31
2.6	Discussion	39

3	A Study of Fiber Excitation Thresholds Using Monopolar and Bipolar Stimulating Electrodes	43
3.1	Introduction	43
3.2	Models	44
3.2.1	First principles model	44
3.2.2	Empirical model	48
3.3	Methods	49
3.3.1	Threshold measurements	49
3.3.2	Data analysis	52
3.4	Results	54
3.4.1	Monopolar threshold vs. distance	54
3.4.2	Bipolar threshold vs. orientation	58
3.5	Discussion	63
3.5.1	Monopolar stimulation	63
3.5.2	Orientation dependence	65
3.5.3	Models	66
3.5.4	Axons or dendrites?	68
3.6	Appendix: Location estimates using the empirical model	69
4	Conclusions	71
4.1	Strengths and weaknesses of new experimental method	71
4.1.1	Stimulating electrode arrays	71
4.1.2	Recording arrays	72
4.1.3	Soma stimulation	72
4.2	Related work re-considered	72
4.3	Implications for epi-retinal prosthesis design	74
5	Future work	77
5.1	Refinements to the present work	77
5.2	Field direction	77
5.3	Pulse duration	79
5.4	Electrode size	79
A	Thresholds for <i>In Vitro</i> Human Retina	82
B	Instrument Designs	85
B.1	Introduction	85
B.2	Stimulator design	85
B.2.1	Isolator	85
B.2.2	Lowpass filters	88
B.2.3	Decoupler circuit	88
B.2.4	Current source	91
B.2.5	Performance specifications	93

B.3	Stimulus monitor amplifier design	94
B.3.1	Differential amplifier	95
B.3.2	Isolation and filters	96
B.3.3	Performance Specifications	97
B.4	Nerve response amplifier design	97
B.4.1	Multiplexer	97
B.4.2	Preamplifier	100
B.4.3	Sample and hold	101
B.4.4	Active lowpass filter	103
B.4.5	High-gain amplifier	103
B.4.6	Bode plot	104
B.5	System considerations	105
B.5.1	Noise	105
B.5.2	Current shunting	111
B.5.3	Summary of ground connections	116
B.6	Dynamic response of current source output network	116
B.6.1	Derivation of transfer function and natural frequencies	118
B.6.2	Interpretation of circuit natural frequencies	119
C	Investigations of Stimulus Artifact	123
C.1	Introduction	123
C.2	Response amplifier considerations	124
C.2.1	Saturation and filters	124
C.2.2	Sample and hold	125
C.2.3	Preamplifier input	125
C.3	Stimulator-amplifier coupling	126
C.4	Stimulator considerations	132
C.4.1	Offsets and supply coupling	132
C.4.2	Series coupling capacitors	133
C.5	Electrode capacitance	133
C.5.1	Stimulating electrodes	133
C.5.2	Recording electrodes	135
C.6	Reducing stimulus artifacts: an overview	136
C.6.1	What to look for	136
C.6.2	What to do	136

List of Figures

1.1	Cross-section of rabbit retina with epi-retinal stimulating electrodes illustrated schematically.	14
2.1	Method for isolating retina from the pigment epithelium.	22
2.2	Head on view of the electrode array.	24
2.3	Array assembly and detailed view of castle-shaped brace.	25
2.4	Cross-section view of the electrode array.	26
2.5	Block diagram of the data acquisition system.	28
2.6	Examples of different spontaneous discharge types.	31
2.7	Overlay of response waveforms for four stimulus amplitudes, before and after addition of 150nM tetrodotoxin.	32
2.8	Response waveforms with an all-or-none component.	33
2.9	Example threshold measurement.	34
2.10	Normalized thresholds vs. phase duration for seven recording sites in seven retinas.	35
2.11	Stimulus and response waveforms for anodic-first and cathodic-first stimulation.	37
2.12	Responses to repetitive supra-threshold stimulation at approximately 500 stimuli/sec.	38
2.13	Map of thresholds for a single unit.	38
2.14	Speculative drawing of the anatomy underlying graded and all-or-none responses.	41
3.1	Activating functions for a point source electrode at a distance D from a fiber.	46
3.2	Bipolar stimulation along fiber and across fiber using a pair of point sources separated by a distance d	47
3.3	Bipolar stimulation.	51
3.4	Relative positions of electrodes and fiber.	52
3.5	Measured data and best-fit theoretical curves for monopolar threshold vs. inferred displacement on the retinal surface, for each of nine fibers. Displacements were inferred using the first principles model.	55

3.6	Measured data and best-fit theoretical curves for monopolar thresholds vs. inferred displacement on the retinal surface, for each of nine fibers. Displacements were inferred using the empirical model.	56
3.7	Monopolar threshold vs. inferred displacement s on the retinal surface (estimated using first principles model).	59
3.8	Normalized bipolar thresholds vs. inferred displacement s (estimated using the first principles model), with theoretical curves superimposed.	60
3.9	Normalized bipolar thresholds vs. inferred displacement s (estimated using the empirical model), with theoretical curves superimposed. . .	61
4.1	Both transretinal and transverse bipolar stimulation produce stimulating fields which run perpendicularly to axons.	73
4.2	Highly schematic comparison of excitation patterns for monopolar and transverse bipolar stimulation.	75
5.1	A stimulating electrode array resembling a tic tac toe board should provide better field uniformity than pairs of $10\mu\text{m}$ diameter disks for measuring thresholds versus field direction.	78
5.2	Array patterns for measuring thresholds versus electrode diameter. . .	80
A.1	Monopolar threshold map for <i>in vitro</i> human retina.	83
B.1	Block diagram representing signal flow in the experimental apparatus.	86
B.2	Block diagram of the stimulator.	86
B.3	Schematic diagram of isolator driver, isolator, and differential to single-ended converter.	87
B.4	Schematic diagram of a generic 2-pole active lowpass filter.	89
B.5	Schematic diagram of circuit used to decouple the stimulator from the noisy isolator output.	90
B.6	Voltage-controlled current source topology.	91
B.7	Voltage-controlled current source and output network.	92
B.8	Block diagram of one stimulus monitor.	95
B.9	Schematic diagram of the differential amplifier at the input of the stimulus monitor.	96
B.10	Eight-channel nerve response recording system.	98
B.11	Block diagram of one nerve response amplifier.	98
B.12	Schematic diagram of multiplexer circuit for electrode selection. . . .	99
B.13	Schematic diagram of the preamplifier circuit.	100
B.14	Schematic diagram of the sample and hold circuit.	101
B.15	Circuit for generating blanking pulses.	102
B.16	Schematic diagram of the high gain amplifier.	103
B.17	Gain and phase plots for nerve response amplifier A.	104
B.18	Schematic diagram of the connected instruments.	106

B.19	Noise voltage measured at the amplifier output with branch 2 (Figure B.18) open and closed.	107
B.20	Connections leading to ground loop pickup from the computer monitor.	109
B.21	Noise voltage measured at the amplifier output with branch 3 open and closed.	110
B.22	Circuit model of the input region of the preamplifier.	112
B.23	Impedance magnitude and phase of electrode D0 on array AEG2.	113
B.24	Possible paths for stimulation current.	114
B.25	Shunt currents with differential recording but a shared ground.	115
B.26	The ground connection scheme used.	117
B.27	Ideal current source and output network.	117
B.28	Fast natural frequency.	120
B.29	Slow natural frequency.	122
C.1	Example stimulus artifact.	124
C.2	Stimulus artifact, with sample and hold circuit activated.	126
C.3	Stimulus artifacts for two bipolar stimulating pairs, symmetrically arranged with respect the the recording electrode.	127
C.4	Stimulus artifacts with and without shielding of the recording electrode.	128
C.5	A SPICE simulation reproduces the stimulus artifact to a fair degree.	130
C.6	Spice model for stimulus artifacts.	131
C.7	Stimulus artifacts with old and new array insulation.	132
C.8	Circuit model for and measurements demonstrating decay transients on stimulating electrodes.	134

List of Tables

1.1	Summary of stimulation parameters for seven studies in which axons were not maximally sensitive.	18
3.1	Curve fit statistics for fiber position estimates using the first principles model.	57
3.2	Curve fits statistics for fiber position estimates using the empirical model.	57
3.3	Comparison of curve fit parameters for the first principles and empirical models.	58
3.4	Summary of thresholds for stimulation at the epi-retinal surface. . . .	64
A.1	Normalized thresholds for horizontal and vertical bipolar stimulation.	83
B.1	Estimated contributions from major sources of noise in amplifier cascade.	111

Chapter 1

Introduction

1.1 Background and motivation

1.1.1 Neural and retinal prostheses

The human body is composed of cells. Our sensory and motor capabilities arise from the properties of various types of nerve and muscle cells, from the complex networks which they form, and from additional supporting cells which maintain a suitable operating environment. Disruption of these cells and networks, caused by disease or injury, can result in paralysis or sensory loss.

Neural prostheses can sometimes compensate for lost function, usually by electrically stimulating viable neurons in pathways where natural connections have been disrupted. Among the most successful examples to date is the cochlear prosthesis, which provides auditory sensation to otherwise profoundly deaf patients. Deafness often results from loss of the hair cells of the inner ear, which transform the mechanical energy of sound into neural signals that can be transmitted to the brain. Cochlear prostheses electrically stimulate surviving neurons which are post-synaptic to the hair cells, effectively bypassing the initial parts of the natural auditory pathway. Prolonged use of cochlear implants can lead to dramatic improvements in both speech perception and speech production, and at present there are at least four different types of commercially available devices (Loizou, 1999).

The visual prosthesis field is less mature. While work on cortically based artificial vision dates back to the 1960's (Hambrecht, 1990), researchers have yet to produce a device ready for routine clinical use. The last decade has seen increasing interest in the development of a retina-based visual prosthesis (Chow and Chow, 1997; Eckmiller, 1997; Humayun et al., 1999; Rizzo and Wyatt, 1997; Zrenner et al., 1999). Unlike cortical prostheses, the success of this approach depends on the survival of at least a subpopulation of retinal neurons. Of critical importance is the survival of the retina's output neurons, the ganglion cells. The degenerative disease retinitis pigmentosa, which affects over a million worldwide (Berson, 1993), fits these criteria. Significant

populations of ganglion and bipolar cells are spared by this disease despite severe photoreceptor loss (Santos et al., 1997; Stone et al., 1992). The primary advantages of a retina-based prosthesis are the surgical accessibility of the ganglion cells and the topographic ordering of their receptive fields. Further consideration of the relative merits of the retinal and cortical approaches is provided elsewhere (Normann et al., 1999; Rizzo and Wyatt, 1997).

This work was undertaken to contribute to the development of a retinal prosthesis which may someday provide useful artificial vision to patients blinded by diseases like retinitis pigmentosa. The prosthesis will function by electrically stimulating healthy inner retinal neurons through a micro-electrode array residing on the retina's exposed surface. The design of such a prosthesis entails many lines of inquiry, including selection of electric stimulation parameters, selection of biocompatible device materials, development of surgical methods for implantation and fixation of the device, electronic design of intra- and extra-ocular components, and design of schemes for transmission of power and signal to the intra-ocular electronics. This thesis is concerned with selection of electric stimulation parameters for the prosthesis.

1.1.2 Electric stimulation parameters

There are a number of free parameters to consider when designing an electric stimulation method, including the shape and size of the stimulating electrodes, the arrangement of the stimulating electrodes on the retina, the wave shape and duration of the stimulation current, and the amplitude of the stimulation current. The plausible parameter space is substantial. While retinal stimulation studies have often used one of a relatively few conventional electrode shapes (e.g. flat circular, flat annular, ball end, sharp point), characteristic dimensions can range from microns to hundreds of microns. In addition, modern micro-fabrication techniques make it possible to pattern flat stimulating electrodes in any desired shape and configuration with micron resolution. Furthermore, a broad range of current waveforms, durations, and amplitudes has been successfully used to stimulate the retina. Current waveforms might range from microseconds to milliseconds in duration and from hundreds of nanoamperes to milliamperes in amplitude.

Coupling between different stimulation variables reduces the useful parameter space to some degree. Over a range of durations, for example, the minimum amplitude capable of eliciting neuronal and perceptual responses will decrease with increasing stimulus duration (i.e. classic strength-duration behavior). On the other hand, the minimum effective amplitude for a particular duration may vary with the shape of the stimulating electrode. Hence many combinations of stimulation parameters will fail to produce retinal responses and, once identified, can be ruled out for use in a prosthesis.

Any candidate set of stimulation parameters must be further judged for its ability to evoke detailed visual sensations, its potential to cause further harm to the retina,

and its total power consumption. The task of the retinal prosthesis designer is to locate optimal regions of the parameter space which maximize performance on the first of these criteria and minimize the latter two.

1.1.3 Objective

The present work aims to elucidate the relationship between the stimulating electrode geometry and the pattern of evoked neuronal responses. The specific objective is motivated by considerations of the interface between the prosthesis and retina, and the types of percepts which might be achievable through such an interface.

The topographic arrangement of receptive fields across the retinal surface lends itself to a simple model of visual perception. Light arriving from a restricted area within the visual scene will activate neurons in a corresponding restricted area on the retinal surface. Conversely, electric stimulation of a small area of retina is expected to result in a focal visual percept. Electrically evoked visual perceptions, or phosphenes, have in fact been demonstrated in numerous experiments (see Section 1.2) with various stimulation methods and degrees of focality. Today's retinal prosthesis designs would employ electrode arrays to gain access to a large number of individually addressable phosphene elements, conveying the visual scene much in the same way that images are represented on a computer screen.

A major concern is that axons in the nerve fiber layer, lying between an epiretinal microelectrode and the target neurons (see Figure 1.1), will be stimulated. Stimulation of axons emanating from ganglion cells far removed from the point of stimulation would probably convey the perception of a peripheral blur, detracting from the usefulness of the imagery. Hence it would be desirable to bypass the axons while selectively stimulating other parts of the ganglion cells and/or other types of surviving cells such as bipolar cells.

Some advantage may be gained from the finding in brain and peripheral nerve experiments that axon thresholds were highest when the stimulating field was oriented perpendicular to the axon's path (Ranck, 1975; Rushton, 1927). This finding is also predicted by theoretical models (Grumet, 1994; Plonsey and Altman, 1988). Thus, a stimulating electrode geometry which limits field components along axon paths might permit selective stimulation of more distant retinal elements. The objective of the present work is to explore this possibility experimentally using an *in vitro* retina preparation.

1.2 Related work

There is a substantial and diverse literature devoted to electric stimulation of the retina. The most recent research was directed, as is this thesis, at retinal prosthesis development. Prior to the 1990's, researchers used electric stimulation either to study

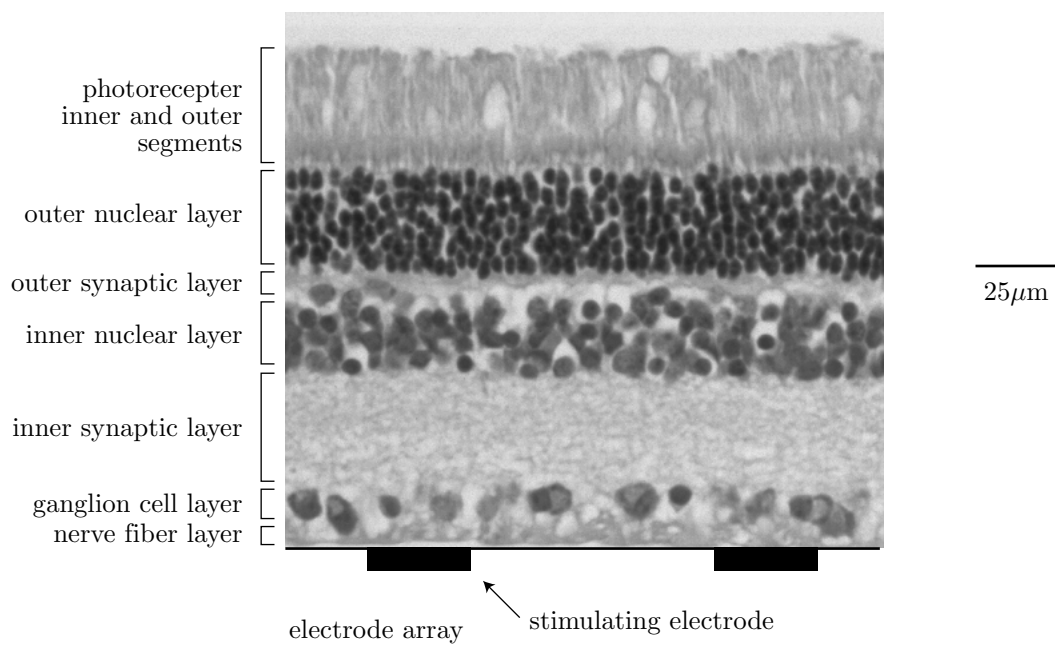


Figure 1.1: Cross-section of rabbit retina with epi-retinal stimulating electrodes illustrated schematically. The section was taken from central retina, a few millimeters below the optic disk. This is the same region that was used for the experiments of Chapters 2 and 3. The retina was stained (with hematoxylin and eosin) and imaged under the direction of Dr. Charles Dangler, D.V.M., Ph.D of MIT's Division of Comparative Medicine.

retinal processing using a novel type of input or to elucidate the excitation mechanisms involved.

Of critical interest when considering this body of work are 1) a comparison of excitation thresholds for ganglion cell axons with thresholds for other retinal elements, and 2) an examination of how the thresholds for axons and other elements depended on the choice of stimulation parameters. This section will concentrate on the threshold comparisons; consideration will be given to absolute thresholds in Chapter 3.

1.2.1 Direct threshold comparisons

Jensen and colleagues (Jensen et al., 1996; Rizzo et al., 1997) and Greenberg (1999) systematically compared excitation thresholds for ganglion cell axons and somata. Using two different stimulating electrode types, monopolar and concentric bipolar, Jensen measured thresholds for producing single spikes in rabbit retinal ganglion cells. Spikes were recorded from each cell's axon at a location near the optic disk. Stimuli were applied in the vicinity of ganglion cell somata and at locations between the somata and recording electrode, along the axon paths. For both stimulating electrode types, median axon thresholds were approximately twice as large as median cell body thresholds. It was also true, however, that cell body and axon thresholds exhibited broad ranges and overlapped substantially.

In contrast with Jensen's experimental work, Greenberg used a computational model to simulate extracellular stimulation of a retinal ganglion cell with a monopolar electrode (Greenberg et al., 1999). In general agreement with Jensen's median threshold data, Greenberg found that thresholds were 20% to 73% higher for axons than for cell bodies.

The stimulation parameters in Jensen's experiments and Greenberg's simulations were similar. In both studies, $100\mu\text{s}$ cathodal stimulation pulses were applied through radially symmetric monopolar electrodes which were placed against the epi-retinal surface. In Jensen's experiments, the electrode had a cone-shaped tip with $5\mu\text{m}$ of exposed length, and the return was an Ag/AgCl sheet placed beneath the sclera. In Greenberg's simulations, the electrode was either a point source, a $50\mu\text{m}$ diameter disk, or a $100\mu\text{m}$ -diameter disk, with the return at infinity. Jensen also used a concentric bipolar stimulating electrode in some experiments. This electrode had a $25\mu\text{m}$ diameter, hemispherical tip and a recessed, annular return with an inner diameter of $200\mu\text{m}$.

1.2.2 Indirect threshold comparisons

In 1977, Dawson and Radtke observed rather usefully that "one would expect most retinal cells to respond at some current level" (Dawson and Radtke, 1977). Hence electrically generated responses might initiate in one type or in many types of retinal neurons, depending on the current level. At current levels which are just sufficient

to produce a retinal output, however, only the element(s) with the lowest excitation thresholds will be directly stimulated. Let's call such elements *maximally sensitive*.

The set of maximally sensitive elements might be a function of the parameters used for stimulation. Also, it might comprise one or more cell types. As illustrated below, studies which identify these maximally sensitive elements permit indirect, semi-quantitative comparisons of thresholds for different retinal elements.

In Jensen's experiments (described above), ganglion cells and their axons were always stimulated directly, as verified from the short and stable response latencies and from the persistence of the responses in the presence of the synaptic blocker cadmium (Jensen, unpublished data). Because no trans-synaptic responses were observed, thresholds for other retinal elements such as bipolar cells and photoreceptors must have been comparatively high. A similar inference cannot be drawn from Greenberg's simulations (also described above), since only ganglion cells were included in the model.

Jensen (1996) also created maps of ganglion cells' electrical receptive fields, as did Greenberg in an experimental study of frog retina (Greenberg, 1998c). The maps were produced by measuring spike thresholds for a large number of stimulating electrode positions in the vicinity of the cell body. In general thresholds increased with distance from a concentrated region of low thresholds, but sometimes there were elongated low-threshold regions extending toward the optic disk. Stimuli were presumably acting on axons in these cases, indicating that axon thresholds were comparatively low.

The stimulation parameters used by Jensen were described in the previous Section. Greenberg (1998c) delivered 0.52ms stimuli to the frog epi-retinal surface through an array of 400 μ m diameter disk electrodes in a variety of monopolar and bipolar configurations. For monopolar stimulation, the return electrode was either placed on the same side of the retina as the stimulating array, several millimeters distant, or else on the opposite (extra-ocular) side of the sclera, directly beneath the stimulating array. Pairs of electrodes with 113 μ m edge-to-edge separation, oriented either in parallel with or perpendicular to the presumed axon path, were used for bipolar stimulation (see Section 1.2.5 for further discussion of these bipolar measurements).

In a number of other accounts, the lowest amplitude stimuli elicited responses whose properties were inconsistent with axon stimulation. Phosphenes elicited in alert human subjects, for example, were localized and corresponded well with electrode positions (Brindley, 1955; Humayun et al., 1996; Humayun et al., 1999). Another phosphene study demonstrated non-linear strength duration curves consistent with an hypothesized interaction of distinct ON and OFF processes (Howarth, 1954). These processes presumably arose within the retinal network. Two additional studies described complex responses which lasted up to two orders of magnitude longer than the originating stimuli (Crapper and Noell, 1963; Doty and Grimm, 1962). Such responses, like Howarth's, probably arose within the retinal network. Finally, a study of *in vitro* frog retina reported on a number of properties of threshold response latencies for ganglion cell spikes (Greenberg, 1998a). Latencies were high (9.8-12.2ms) in nor-

mal retinal and low (3.7ms) in the presence of the synaptic blocker cadmium. More interestingly, the latencies in normal retina fell with increasing current level until a discontinuous jump in latency occurred from 6-7ms to 3-4ms. The lower-threshold, higher-latency responses were consistent with stimulation of elements pre-synaptic to ganglion cells, whereas the higher-threshold, lower-latency responses arose in ganglion cells or their axons. Two of the other studies mentioned above (Crapper and Noell, 1963; Doty and Grimm, 1962) also described a similar duality of response types. Though not maximally sensitive in these studies, axons may have been stimulated at thresholds which were only slightly higher than the thresholds for other elements.

Stimulation parameters for these seven studies are summarized in Table 1.1.

1.2.3 The pulse duration hypothesis

Greenberg (1998b) argued that ganglion cell stimulation—at the axon or otherwise—can be avoided completely by using sufficiently long (>.5ms) stimulation pulses. Primary support for this claim came from a series of strength-duration curves for ganglion cell spikes in the frog retina. To isolate direct ganglion cell stimulation from stimulation of deeper cells, Greenberg measured some of the strength-duration curves in the presence of the synaptic blocker cadmium. The stimulating electrode type and placement, which were identical to those used in another study (Greenberg, 1998a), are listed in Table 1.1.

Addition of cadmium to the bathing medium raised the rheobase and lowered the chronaxie relative to normal retina. In addition, the strength duration curves for normal retina, which were measured under both light and in the dark conditions, intersected the cadmium curve such that thresholds under cadmium were relatively high for long stimulation pulses and relatively low for short pulses. Hence ganglion cells would be expected to be maximally sensitive at short pulse durations whereas other retinal elements would be maximally sensitive at longer pulse durations. Support for this hypothesis came from a phosphene experiment in which a 0.7mm disk was placed against a blind patient's retina and the pulse duration varied. Phosphenes were relatively focal for 1-8ms durations but became elongated when the pulse duration was lowered to 0.5ms.

Two alternative numerical substitutes for the boundary between “short” and “long” can be determined from the durations at which strength-duration curves for normal and cadmium conditions intersected. These were roughly 0.1ms for dark-adapted retina and 3ms for light-adapted retina. The 0.5ms boundary suggested by Greenberg falls between these intersection points, and comes apparently from the phosphene experiment. With one exception (Brindley, 1955), the studies in Table 1.1 are consistent the Greenberg's hypothesis since stimuli were 0.5ms or greater and axon thresholds were comparatively high.

Study	Response type (species)	Stimulus phase duration	Electrode type	Electrode placement
Brindley (1955)	Phosphenes (human)	a few μs – DC	Various monopolar and bipolar, several mm long	Against the conjunctiva; monopolar return in mouth
Crapper & Noell (1963)	GC spikes (rabbit)	0.5ms	Monopolar	Vitreous; return under the skin overlying the sacrum
Doty & Grimm (1962)	Cortical potentials (cat)	1ms	Bipolar, 1mm separation	Epi-retinal surface; various orientations relative to axons
Greenberg (1998a)	GC spikes (frog)	0.52ms	Monopolar, 1.5mm diameter	Scleral surface; return several mm distant on epi-retinal side
Howarth (1954)	Phosphenes (human)	7–100ms	Monopolar	Forehead; return in hand
Humayun (1996)	Phosphenes (human)	1–4ms	Various monopolar & bipolar, 50-200 μm diameter	500 μm above epi-retinal surface; monopolar return at a distant location
Humayun (1999)	Phosphenes (human)	$\leq 2\text{ms}$	Arrays: 400 μm disks; monopolar & bipolar Wire electrodes: 25–125 μm disks; monopolar & bipolar	Epi-retinal surface; monopolar return on shoulder 500 μm above epi-retinal surface; monopolar return on shoulder

Table 1.1: Summary of stimulation parameters for seven studies in which axons were not maximally sensitive. Excitation thresholds for a number of studies—one appearing in this table and several mentioned in the text—are listed in Table 3.4. *Abbreviations:* GC = ganglion cell.

1.2.4 Other studies

A number of studies not described above are equivocal for the purpose of comparing thresholds for axons and other retinal elements. Several researchers, for example, recorded exclusively from retinal neurons which preceded ganglion cells in the visual pathway and would not have observed responses arising in axons, had they occurred (Miyachi et al., 1984; Murakami et al., 1982; Toyoda and Fujimoto, 1984; Trifonov and Byzov, 1977). Ogden and Brown, on the other hand, recorded antidromic ganglion cell spikes and several other types of responses at various retinal depths, but did not determine the thresholds for these (Ogden and Brown, 1964). In still other studies, recordings were made from or subsequent to ganglion cells, and stimulation thresholds determined as well, but initial excitation sites were not identified (Dawson and Radtke, 1977; Humayun et al., 1994). Finally, a number of researchers demonstrated complex responses *in vitro* which, like Howarth's, probably arose in the retinal network, but did not (or had no reason to) convincingly rule out the possibility that axons were stimulated directly as well (Gernandt and Granit, 1947; Granit, 1946; Granit, 1948; Knighton, 1975; Molotchnikoff, 1976; Molotchnikoff and Lachapelle, 1978; Potts and Inoue, 1970).

1.2.5 Discussion

In numerous experiments and in one computational study, excitation thresholds were generally higher for axons than for other retinal elements. However, in most of these studies the stimulating electrodes were not placed against the epi-retinal surface, as they would be in an eventual implant. As discussed further in Section 4.2, this realistic configuration is also particularly well-suited for axon stimulation. Where stimuli were applied to the epi-retinal surface and direct threshold comparisons for axons and other elements (specifically, ganglion cell bodies) were made, thresholds for the two groups showed broad overlap, with median thresholds for the former no more than twice as large as median thresholds for the latter.

The margin of axon thresholds above other elements' thresholds might be substantially raised using electrode designs which produce stimulating fields running perpendicularly to axons. This hypothesis has not been systematically tested in retina, though a few measurements suggestive of it were made by Greenberg (1998c) using bipolar electrodes at the epi-retinal surface in frogs. Consistent with the hypothesis, axon stimulation was never observed when the bipolar electrode pair was oriented perpendicular to the presumed axon path (N=2 cells). Furthermore, axon stimulation did occur in one of the two cases where the bipolar pair was oriented in parallel with the presumed axon path. However, the axon locations relative to the stimulating electrodes—which was found in the present work to strongly influence the dependence of axon thresholds on the orientation of the bipolar pair—were neither known nor estimated.

1.3 What's In This Thesis

In pursuit of the goal described above, I constructed a new experimental apparatus and conducted experiments on isolated rabbit retinas. The setup employed micro-fabricated electrode arrays, which allowed rapid switching between different electrode configurations without mechanical disruption of the tissue, and provided tremendous flexibility in patterning electrode shapes and arrangements. Axon (and possibly dendrite) excitation thresholds were measured using $10\mu\text{m}$ diameter disk stimulating electrodes, both singly versus a distant return (monopolar stimulation) and in pairs (bipolar stimulation). Bipolar electrode pairs were oriented across the fibers under study (transverse orientation) and along the fibers (longitudinal orientation). Thresholds for transverse bipolar stimulation were compared with those for monopolar and longitudinal bipolar stimulation at the same distance from the fiber. Transverse thresholds were greater than monopolar or longitudinal thresholds, provided that the target fiber was near the midpoint between the two electrodes used for transverse bipolar stimulation. The ratio of transverse to longitudinal thresholds was close to unity if one of the electrodes forming the bipolar pair was directly over the fiber, and rose rapidly as the fiber approached the midpoint. The largest measured ratio was about 3.5. These results are consistent with theory and previous experiments, since thresholds were highest when the stimulating field was most nearly perpendicular to fibers, but show that bipolar electrode pairs formed from $10\mu\text{m}$ diameter disks would not be optimal for use in a retinal prosthesis.

The remainder of the thesis is structured as follows:

Chapter 2 describes the method developed to stimulate and record from patches of isolated retina using a planar microelectrode array.

Chapter 3 describes measurements of thresholds for generating single spikes in fibers using monopolar and bipolar stimulating electrodes.

Chapter 4 considers the strengths and weaknesses of the new experimental methods, and comments on the implications of the thesis results for the design of an epiretinal prosthesis.

Chapter 5 puts forth some thoughts for future work.

Appendix A presents data from one set of measurements where thresholds were determined for an *in vitro* human retina.

Appendix B provides detail on the design of custom electronic instruments used in the experimental setup.

Appendix C summarizes efforts to reduce stimulus artifacts.